COEFFICIENT-TRUNCATED HIGHER-ORDER COMMUTING MATRICES OF THE DISCRETE FOURIER TRANSFORM

Soo-Chang Pei, Wen-Liang Hsue, and Jian-Jiun Ding

Graduate Institute of Communication Engineering, National Taiwan University, Taipei, Taiwan, R.O.C.

Email address: pei@cc.ee.ntu.edu.tw

ABSTRACT

Recently, Candan introduced higher order DFT-commuting matrices whose eigenvectors are accurate approximations to the continuous Hermite-Gaussian functions (HGFs). However, the highest order $2k$ of the $O(h^{2k})$ $N\times N$ DFT-commuting matrices proposed by Candan is restricted by $2k+1\leq N$. In this paper, we remove that restriction of order upper bound by developing a coefficient truncation technique to construct arbitrary-order DFT-commuting matrices. Exploiting that coefficient truncation technique, we also develop a method to construct n-diagonal arbitrary-order DFT-commuting matrices, whose number of nonzero diagonal bands n can be prespecified at will. Results of computer experiments show that the Hermite-Gaussian-like (HGL) eigenvectors of the new DFT-commuting matrices proposed in this paper outperform those of Candan's.

***Index Terms*—**commuting matrix, discrete Fourier transform, Hermite-Gaussian function, discrete fractional Fourier transform, eigenvector

1. INTRODUCTION

1.1 Previous Works on DFT-Commuting Matrices

The discrete fractional Fourier transform (DFRFT) is the fractional version of the discrete Fourier transform (DFT). In order to define DFRFT whose outputs are sample approximations of the continuous fractional Fourier transform, generations of HGL DFT-eigenvectors are important for this kind of DFRFT definitions [1]-[2]. In [1], the DFRFT is defined based on HGL eigenvectors computed from the Dickinson-Steiglitz extended-tridiagonal commuting matrix of the DFT [3]. Pei et al. [2] proposed another extended-tridiagonal DFT-commuting matrix whose eigenvectors are closer to the continuous HGFs than those of the Dickinson-Steiglitz matrix. Recently, Candan [4] proposed the higher order DFT-commuting matrices whose eigenvectors approximate the continuous HGFs even more accurately than those of the Dickinson-Steiglitz matrix [3] and those of the DFT-commuting matrices introduced in [2]. Possible applications of the fractional Fourier transform in the signal processing area include optimal filtering [5], data encryption [6], etc.

1.2 Continuous Hermite-Gaussian Functions (HGFs)

The continuous HGFs are eigenfunctions of the continuous Fourier transform and are solutions of the following second-order differential equation [7]:

$$\frac{d^2}{dt^2}f(t)-4\pi^2t^2f(t)=\lambda\cdot f(t)\,. \tag{1}$$

It is shown in [1] that (1) can also be expressed as:

$$\mathcal{S}\{f(t)\}=\lambda\cdot f(t)\text{, where} \tag{2}$$

$$\mathcal{S}\equiv\mathcal{D}^2+\mathcal{F}\mathcal{D}^2\mathcal{F}^{-1} \tag{3}$$

with $\mathcal{D}$ and $\mathcal{F}$ being the differentiation operator and the continuous Fourier transform operator, respectively. Therefore, the HGFs are also eigenfunctions of the operator $\mathcal{S}$ defined in (3).

1.3 General DFT-Commuting Matrices

The $N\times N$ DFT matrix $\mathbf{F}$ is defined as

$$[\mathbf{F}]_{kn}=\frac{1}{\sqrt{N}}e^{-j\frac{2\pi}{N}kn},\quad 0\leq k,n\leq N-1\,. \tag{4}$$

It is shown in [4] that any $N\times N$ DFT-commuting matrix $\mathbf{A}$ can be expressed as:

$$\mathbf{A}=\mathbf{L}+\mathbf{FLF}^{-1}+\mathbf{F}^2\mathbf{LF}^{-2}+\mathbf{F}^3\mathbf{LF}^{-3}\,, \tag{5}$$

where $\mathbf{L}$ is an arbitrary $N\times N$ matrix. In fact, the general form of the DFT-commuting matrix in (5) can be further simplified as follows.

Definition: An $N\times N$ matrix $\mathbf{B}$ is defined to be $\mathbf{K}$-symmetric if [8]

$$\mathbf{KBK}=\mathbf{B}, \tag{6}$$

where $\mathbf{K}$ is the circular reversal matrix given by

$$\mathbf{K}\equiv\mathbf{F}^2=\begin{bmatrix}1 & \mathbf{0}\\ \mathbf{0} & \mathbf{J}\end{bmatrix}_{N\times N} \tag{7}$$

with $\mathbf{J}$ being the $(N-1)\times(N-1)$ reversal matrix whose nonzero entries are ones on the antidiagonal. An $N\times 1$ vector $\mathbf{x}$ is defined to be $\mathbf{K}$-symmetric if $\mathbf{Kx}=\mathbf{x}$.

Property 1: Let us define an $N\times N$ matrix $\mathbf{S}$ as:

$$\mathbf{S}=\mathbf{M}+\mathbf{FMF}^{-1} \tag{8}$$

where $\mathbf{M}$ is an $N\times N$ $\mathbf{K}$-symmetric matrix. Then $\mathbf{S}$ commutes with $\mathbf{F}$.

Proof: $\mathbf{FS}=\mathbf{FM}+\mathbf{F}^2\mathbf{MF}^{-1}=\mathbf{FM}+\mathbf{F}^2\mathbf{MF}^{-2}\mathbf{F}$
$=\mathbf{FM}+\mathbf{KMKF}=\mathbf{FM}+\mathbf{MF}=\mathbf{SF}$. #

From *Property 1*, a DFT-commuting matrix $\mathbf{S}$ can be constructed by first choosing a $\mathbf{K}$-symmetric generating matrix $\mathbf{M}$ and then substituting it into (8).

1.4 Candan's Higher Order DFT-Commuting Matrices

The $(2k)^{\text{th}}$-order approximation to the second derivative is derived by Candan [4], [9] and is:

$$f''(x_k)=\left(\sum_{m=1}^{k}(-1)^{m-1}\frac{2[(m-1)!]^2}{(2m)!}\delta^{2m}\right)\frac{f_k}{h^2}+O(h^{2k})\,, \tag{9}$$

where $\delta^2 f_k\equiv f_{k+1}-2f_k+f_{k-1}$ is the second central differencing. Equation (9) is used by Candan [4] to derive the $O(h^{2k})$ DFT-commuting matrix. For example, from (9), the $O(h^4)$ approximation of the second derivative is

$$f''(x_k)=\frac{1}{h^2}\left(-\frac{1}{12}f_{k+2}+\frac{4}{3}f_{k+1}-\frac{5}{2}f_k+\frac{4}{3}f_{k-1}-\frac{1}{12}f_{k-2}\right). \tag{10}$$

According to the work of Candan [4], the $O(h^4)$ 7×7 generating matrix $\mathbf{M}_4$ which approximates the second derivative can then be constructed by circularly shifting the $O(h^4)$ coefficient series {-1/12, 4/3, -5/2, 4/3, -1/12} in (10) as follows. First, define the $O(h^4)$ 1×7 generating vector $\mathbf{m}_4$ as:

$$\mathbf{m}_4=[-5/2, 4/3, -1/12, 0, 0, -1/12, 4/3]. \tag{11}$$

Then the $O(h^4)$ 7×7 generating matrix $\mathbf{M}_4$ is [4]:

$$\mathbf{M}_4 = \begin{bmatrix} \mathbf{m}_4(0) \\ \mathbf{m}_4(1) \\ \vdots \\ \mathbf{m}_4(6) \end{bmatrix} = \begin{bmatrix} -5/2 & 4/3 & -1/12 & 0 & 0 & -1/12 & 4/3 \\ 4/3 & -5/2 & 4/3 & -1/12 & 0 & 0 & -1/12 \\ -1/12 & 4/3 & -5/2 & 4/3 & -1/12 & 0 & 0 \\ 0 & -1/12 & 4/3 & -5/2 & 4/3 & -1/12 & 0 \\ 0 & 0 & -1/12 & 4/3 & -5/2 & 4/3 & -1/12 \\ -1/12 & 0 & 0 & -1/12 & 4/3 & -5/2 & 4/3 \\ 4/3 & -1/12 & 0 & 0 & -1/12 & 4/3 & -5/2 \end{bmatrix} \tag{12}$$

where $\mathbf{m}_4(p)$ is obtained from $\mathbf{m}_4$ by circularly shifting it p positions to the right. Substituting $\mathbf{M}_4$ in (12) into (8), the $O(h^4)$ DFT-commuting matrix $\mathbf{S}_4$ can be obtained. From (8) and (3), the resulting DFT-commuting matrix $\mathbf{S}_4$ is a discrete approximation of the continuous HGF generating operator $\mathcal{S}$ in (3) and thus $\mathbf{S}_4$ has HGL eigenvectors. In [4], Candan showed that the eigenvectors of higher order DFT-commuting matrices are closer to HGFs than those of the lower order ones. From (9), the length of the coefficient series for $O(h^{2k})$ approximation to the second derivative is $2k+1$. Therefore, it is important to notice that in Candan's work the highest order $2k$ of the $N\times N$ $O(h^{2k})$ DFT-commuting matrix is restricted by $2k+1\leq N$, such that the length-$(2k+1)$ coefficient series for (9) can be accommodated into the rows of the $N\times N$ generating matrix $\mathbf{M}$.

2. COEFFICIENT-TRUNCATED ARBITRARY-ORDER DFT-COMMUTING MATRICES

In this section, we will modify Candan's work in [4] by proposing arbitrary-order DFT-commuting matrices using a coefficient truncation technique.

Before introducing the coefficient truncation technique to construct arbitrary-order DFT-commuting matrices, we first observe the distribution of coefficient series for $O(h^{2k})$ approximation to the second derivative in (9). For example, from (10), the $O(h^4)$ coefficient series are {-1/12, 4/3, -5/2, 4/3, -1/12}. From this 4^{th}-order coefficient series and coefficient series of other orders, we find that the absolute values of the $O(h^{2k})$ coefficients near the central positions are larger and are dominant coefficients for all k.

According to the above observation, we propose the $O(h^{2k})$ $N\times N$ DFT-commuting matrices using a coefficient truncation technique as follows. For the following discussions in this section, we assume that $2k+1>N$. Because $2k+1>N$, Candan's method in [4] cannot be directly applied for this case. However, because the central coefficients of the coefficient series for $O(h^{2k})$ approximation to the second derivative in (9) are dominant coefficients, we can use only the central N dominant coefficients to construct the generating matrix and set all of the remaining minor coefficients as zeros. Therefore, assume that the $O(h^{2k})$ coefficient series for (9) are $\{a_k, a_{k-1}, \ldots, a_1, a_0, a_1, \ldots, a_k\}$. Then the $1\times N$ $O(h^{2k})$ coefficient-truncated generating vector $\mathbf{m}_{2k,N}$ can be constructed as:

$$\mathbf{m}_{2k,N} = \begin{cases} [a_0, a_1, \ldots, a_\upsilon, a_\upsilon, a_{\upsilon-1}, \ldots, a_1], \text{if } N \text{ is odd}, \\ [a_0, a_1, \ldots, a_\upsilon, a_{\upsilon-1}, \ldots, a_1], \text{if } N \text{ is even}, \end{cases} \tag{13}$$

where $\upsilon=\left\lfloor \frac{N}{2} \right\rfloor$. In (13), the first subscript $2k$ indicates that the generating vector $\mathbf{m}_{2k,N}$ is constructed from the $O(h^{2k})$ approximation to the second derivative in (9) and the second subscript N indicates that the length-$(2k+1)$ coefficients series for (9) are truncated to reserve only the central N dominant coefficients. With the generating vector $\mathbf{m}_{2k,N}$ in (13), the corresponding $O(h^{2k})$ $N\times N$ generating matrix $\mathbf{M}_{2k,N}$ can be easily constructed as:

$$\mathbf{M}_{2k,N} = \begin{bmatrix} \mathbf{m}_{2k,N}(0) \\ \mathbf{m}_{2k,N}(1) \\ \vdots \\ \mathbf{m}_{2k,N}(N-1) \end{bmatrix}, \tag{14}$$

where $\mathbf{m}_{2k,N}(p)$ is obtained from $\mathbf{m}_{2k,N}$ by circularly shifting it p positions to the right. $\mathbf{M}_{2k,N}$ in (14) is $\mathbf{K}$-symmetric because $(\mathbf{m}_{2k,N})^T$ is $\mathbf{K}$-symmetric, with T being the transpose operation. Consequently, $\mathbf{M}_{2k,N}$ is a valid generating matrix. Then the corresponding $O(h^{2k})$ $N\times N$ DFT-commuting matrix $\mathbf{S}_{2k,N}$ can be computed by substituting $\mathbf{M}_{2k,N}$ in (14) into (8).

For example, the $O(h^{10})$ 7×7 generating matrix $\mathbf{M}_{10,7}$ can be constructed as follows. Assume that the coefficient series for the $O(h^{10})$ approximation to the second derivative in (9) is $\{b_5, b_4, b_3, b_2, b_1, b_0, b_1, b_2, b_3, b_4, b_5\}$. This length-11 coefficient series can then be truncated to a length-7 dominant coefficient series as $\{b_3, b_2, b_1, b_0, b_1, b_2, b_3\}$. From (13), the $O(h^{10})$ 1×7 generating vector $\mathbf{m}_{10,7}$ is:

$$\mathbf{m}_{10,7}=[b_0, b_1, b_2, b_3, b_3, b_2, b_1]. \tag{15}$$

Therefore, from (14), the $O(h^{10})$ 7×7 generating matrix $\mathbf{M}_{10,7}$ is:

$$\mathbf{M}_{10,7} = \begin{bmatrix} \mathbf{m}_{10,7}(0) \\ \mathbf{m}_{10,7}(1) \\ \vdots \\ \mathbf{m}_{10,7}(6) \end{bmatrix} = \begin{bmatrix} b_0 & b_1 & b_2 & b_3 & b_3 & b_2 & b_1 \\ b_1 & b_0 & b_1 & b_2 & b_3 & b_3 & b_2 \\ b_2 & b_1 & b_0 & b_1 & b_2 & b_3 & b_3 \\ b_3 & b_2 & b_1 & b_0 & b_1 & b_2 & b_3 \\ b_3 & b_3 & b_2 & b_1 & b_0 & b_1 & b_2 \\ b_2 & b_3 & b_3 & b_2 & b_1 & b_0 & b_1 \\ b_1 & b_2 & b_3 & b_3 & b_2 & b_1 & b_0 \end{bmatrix}. \tag{16}$$

It is easy to verify that $\mathbf{M}_{10,7}$ is $\mathbf{K}$-symmetric from the definition (6).

Computer Experiment 1: First, we compute the HGL eigenvectors of the 32×32 DFT-commuting matrices of 2^{nd}-order ($\mathbf{S}_2$), 30^{th}-order ($\mathbf{S}_{30}$), and coefficient-truncated 200^{th}-order ($\mathbf{S}_{200,32}$). Fig. 1(a) plots the error norms for the HGL eigenvectors of those DFT-commuting matrices. Log scales of the same results are plotted in Fig. 1(b). In fact, $\mathbf{S}_{30}$ is the highest-order 32×32 DFT-commuting matrix in Candan's work [4], and $\mathbf{S}_2$ is the Dickinson-Steiglitz matrix [3]. From Fig. 1, the eigenvectors of higher order DFT-commuting matrices are closer to samples of HGFs than those of the lower order ones, as expected. Most of the HGL eigenvectors of $\mathbf{S}_{200,32}$ outperform those of $\mathbf{S}_{30}$. The total error norms of HGL eigenvectors in Fig. 1 for $\mathbf{S}_{200,32}$ and $\mathbf{S}_{30}$ are 5.8285 and 7.2127, respectively. In Fig. 1(b), the HGL eigenvectors of $\mathbf{S}_{200,32}$ with smaller numbers of zero-crossings degrade because of the coefficient truncation. However, those degradations are negligible.

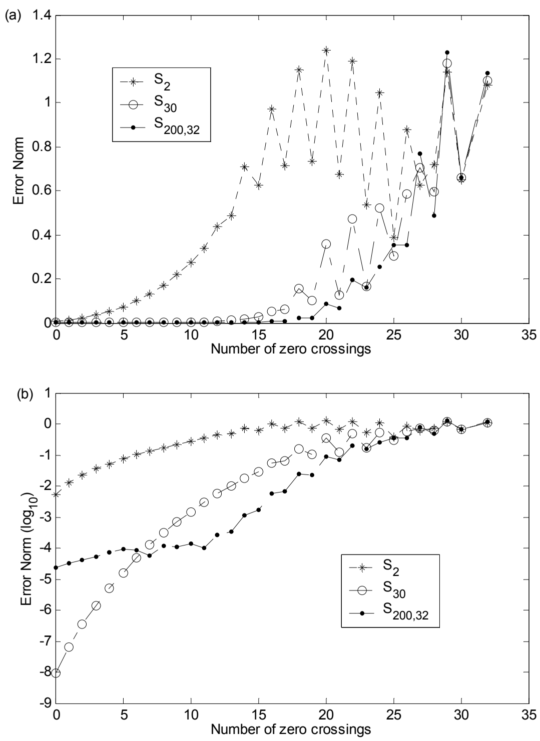

Fig. 1. Error norms for HGL eigenvectors of 32×32 DFT-commuting matrices of 2nd-order ($\mathbf{S}_2$), 30th-order ($\mathbf{S}_{30}$), and coefficient-truncated 200th-order ($\mathbf{S}_{200,32}$). (a) Normal scale. (b) Log scale.

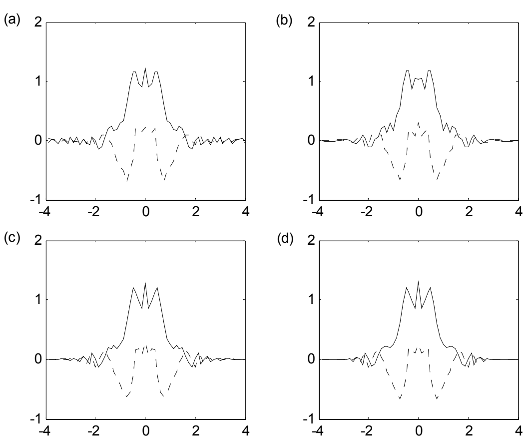

Fig. 2. Transform results of the continuous fractional Fourier transform as well as the 64-point DFRFTs based on the 64×64 DFT-commuting matrix of 2nd-order ($\mathbf{S}_2$), 62th-order ($\mathbf{S}_{62}$), and coefficient-truncated 500th-order ($\mathbf{S}_{500,64}$) for a rectangular signal (real parts: solid lines, imaginary parts: dashes, fractional order=0.25). (a) Continuous fractional Fourier transform; (b) DFRFT based on $\mathbf{S}_2$ (RMSE=0.0913); (c) DFRFT based on $\mathbf{S}_{62}$ (RMSE=0.0519); (d) DFRFT based on $\mathbf{S}_{500,64}$ (RMSE=0.0466).

Next, in Fig. 2, we plot the continuous fractional Fourier transform as well as the 64-point DFRFTs [2] for the following rectangular signal:

$$x(t) = 1 \text{ when } |t| \le 17/16, \qquad x(t) = 0 \text{ elsewhere.} \tag{17}$$

All of the fractional orders for Figs. 2(a)-(d) are 0.25. The DFRFTs in Figs. 2(b)-(d) for samples of $x(t)$ in (17) are computed with sampling interval 1/8. Note that $\mathbf{S}_{62}$ used for Fig. 2(c) is the highest-order 64×64 DFT-commuting matrix in Candan's work [4]. From Fig. 2, the DFRFT based on DFT-commuting matrix of higher order is more similar to the continuous fractional Fourier transform than that of lower order, in the sense of smaller RMSE (root-mean-square error).

3. THE *n*-DIAGONAL ARBITRARY-ORDER DFT-COMMUTING MATRICES

Although the HGL eigenvectors computed from the lower order DFT-commuting matrices have larger error norms [4], the lower order DFT-commuting matrices have the advantage of sparse matrix structures which can be exploited to reduce the computations of their eigenvectors. For example, the $O(h^4)$ 7×7 DFT-commuting matrix $\mathbf{S}_4$ can be derived by substituting the generating matrix $\mathbf{M}_4$ in (12) into (8) and is given in [1]. From (12) and the explicit expression of $\mathbf{S}_4$ in [1], we know that $\mathbf{M}_4$ and $\mathbf{S}_4$ are both 5-diagonal. In this paper, a matrix is called *n*-diagonal if its nonzero entries are at the *n*-diagonal or the extended *n*-diagonal entries. As another example, the $O(h^2)$ DFT-commuting matrix $\mathbf{S}_2$ is 3-diagonal [1]. In this section, we will use the coefficient truncation technique to develop *n*-diagonal arbitrary-order $O(h^{2k})$ DFT-commuting matrices whose eigenvectors are closer to continuous HGFs than those of the *n*-diagonal DFT-commuting matrix introduced by Candan in [4].

In Sec. 2, the coefficient series with length $2k+1$ for the $O(h^{2k})$ approximation to the second derivative in (9) are truncated to the dominant coefficient series of length N, in order that the $N\times N$ generating matrix $\mathbf{M}$ can accommodate them. In fact, the length-$(2k+1)$ coefficient series for (9) can be truncated to a new coefficient series of odd length n, which is even smaller than N. The resulting $O(h^{2k})$ generating matrix based on this new truncated coefficient series of length n will be *n*-diagonal as follows. Let us assume that $n=2s+1$, and the $O(h^{2k})$ coefficient series for (9) are $\{a_k, a_{k-1}, \ldots, a_1, a_0, a_1, \ldots, a_k\}$. Then the truncated dominant coefficient series with length n are $\{a_s, a_{s-1}, \ldots, a_1, a_0, a_1, \ldots, a_s\}$ with $n<N$. The $O(h^{2k})$ generating vector based on this truncated coefficient series is given by:

$$\mathbf{m}_{2k,n} = [a_0, a_1, \ldots, a_s, 0, \ldots, 0, a_s, a_{s-1}, \ldots, a_1]_{1\times N} \tag{18}$$

where the second subscript n indicates that the length-$(2k+1)$ coefficient series for (9) are truncated to reserve only the n central dominant coefficients. With $\mathbf{m}_{2k,n}$ in (18), the *n*-diagonal $N\times N$ $O(h^{2k})$ generating matrix $\mathbf{M}_{2k,n}$ can be easily constructed as:

$$\mathbf{M}_{2k,n} = \begin{bmatrix} \mathbf{m}_{2k,n}(0) \\ \mathbf{m}_{2k,n}(1) \\ \vdots \\ \mathbf{m}_{2k,n}(N-1) \end{bmatrix}. \tag{19}$$

From (8), the $N\times N$ DFT-commuting matrix $\mathbf{S}_{2k,n}$ corresponding to $\mathbf{M}_{2k,n}$ is:

$$\mathbf{S}_{2k,n} = \mathbf{M}_{2k,n} + \mathbf{F}\mathbf{M}_{2k,n}\mathbf{F}^{-1}. \tag{20}$$

Property 2: The $N\times N$ DFT-commuting matrix $\mathbf{S}_{2k,n}$ in (20) is *n*-diagonal.

In fact, the explicit expression of the n-diagonal $N \times N$ $O(h^{2k})$ DFT-commuting matrix $\mathbf{S}_{2k,n}$ is given by

$\mathbf{S}_{2k,n} = \mathbf{M}_{2k,n} + diag(d_0, d_1, \ldots, d_{N-1})$, (21)

where $\mathbf{M}_{2k,n}$ is given by (19), and d_0, d_1, …, d_{N-1} are given by

$$d_\mu = a_0 + \sum_{\alpha=1}^{s} 2a_\alpha \cos(\alpha \cdot \mu \cdot \tfrac{2\pi}{N}) . \quad (22)$$

Using the notation of this section, the n-diagonal $N \times N$ DFT-commuting matrix in Candan [4] is $\mathbf{S}_{n-1,n}$ because its order is fixed and is n-1 (i.e., there is no truncation for the coefficient series), where n is odd and $n \le N$.

Computer Experiment 2: In Fig. 3, we plot the error norms for HGL eigenvectors of the 7-diagonal 200th-order 32×32 DFT-commuting matrix $\mathbf{S}_{200,7}$. For comparison, the HGL eigenvectors for the corresponding 7-diagonal 6th-order 32×32 DFT-commuting matrix (without coefficient truncation) $\mathbf{S}_6$ of Candan [4] are also plotted in Fig. 3. From Fig. 3, we find that most of the HGL eigenvectors computed from $\mathbf{S}_{200,7}$ outperform those computed from $\mathbf{S}_6$ because the former uses larger order to approximate the second derivative. The total error norms of $\mathbf{S}_{200,7}$ and $\mathbf{S}_6$ in Fig. 3 are 8.1323 and 12.3895, respectively. However, compared with $\mathbf{S}_6$, HGL eigenvectors with fewer zero-crossings for $\mathbf{S}_{200,7}$ degrade because of the coefficient truncation. Fig. 3 also plots the error norms of HGL eigenvectors for 15-diagonal 32×32 DFT-commuting matrices of order 200 ($\mathbf{S}_{200,15}$) and of order 14 ($\mathbf{S}_{14}$). From Fig. 3, most of the eigenvectors of $\mathbf{S}_{200,15}$ are closer to HGFs than those of $\mathbf{S}_{14}$, again because the former is of higher order. Total error norms of $\mathbf{S}_{200,15}$ and $\mathbf{S}_{14}$ are 6.0688 and 9.0638, respectively. Besides, compared with $\mathbf{S}_{200,7}$, the degradations for HGL eigenvectors with fewer zero-crossings of $\mathbf{S}_{200,15}$ are very small because more dominant coefficients are reserved for $\mathbf{S}_{200,15}$ than for $\mathbf{S}_{200,7}$.

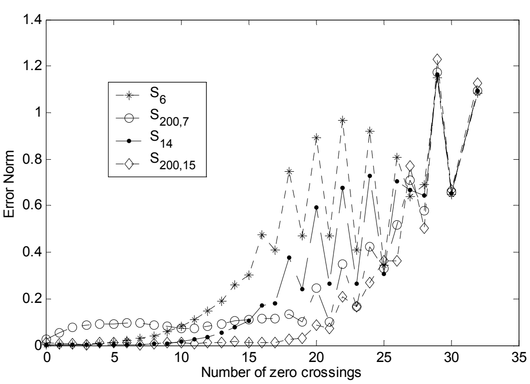

Fig. 3. Error norms for HGL eigenvectors of 7-diagonal DFT-commuting matrices of order 6 ($\mathbf{S}_6$) and of order 200 ($\mathbf{S}_{200,7}$), as well as 15-diagonal DFT-commuting matrices of order 14 ($\mathbf{S}_{14}$) and of order 200 ($\mathbf{S}_{200,15}$), N=32.

It should be noted that the coefficient truncation technique in this section can not be used to reduce the error norms for the HGL eigenvectors of the 3-diagonal $N \times N$ $O(h^{2k})$ DFT-commuting matrix $\mathbf{S}_{2k,3}$, which is explained as follows. Let the $1 \times N$ generating vector of $\mathbf{S}_{2k,3}$ be

$$\mathbf{m}_{2k,3} = [a_0, a_1, 0, \ldots, 0, a_1] . \quad (23)$$

Then the corresponding 3-diagonal $N \times N$ $O(h^{2k})$ generating matrix is $\mathbf{M}_{2k,3} = a_0\mathbf{I} + a_1\mathbf{I}_1$, where $\mathbf{I}$ is the identity matrix and $\mathbf{I}_1$ is given by

$$\mathbf{I}_1 = \begin{bmatrix} \mathbf{e}_1(0) \\ \mathbf{e}_1(1) \\ \vdots \\ \mathbf{e}_1(N-1) \end{bmatrix}, \quad (24)$$

with $\mathbf{e}_1 = [0,1,0,\cdots,0,1]_{1 \times N}$. (25)

Therefore,

$$\mathbf{S}_{2k,3} = \mathbf{M}_{2k,3} + \mathbf{F}\mathbf{M}_{2k,3}\mathbf{F}^{-1} = (a_0\mathbf{I} + a_1\mathbf{I}_1) + (a_0\mathbf{I} + a_1\mathbf{F}\mathbf{I}_1\mathbf{F}^{-1}) = 2a_0\mathbf{I} + a_1(\mathbf{I}_1 + \mathbf{F}\mathbf{I}_1\mathbf{F}^{-1}), \quad (26)$$

where $\mathbf{I}_1 + \mathbf{F}\mathbf{I}_1\mathbf{F}^{-1}$ is the Dickinson-Steiglitz matrix [3]. From (26), $\mathbf{S}_{2k,3}$ and $(\mathbf{I}_1 + \mathbf{F}\mathbf{I}_1\mathbf{F}^{-1})$ have the same eigenvector set for all k.

4. CONCLUSION

In this paper, we extended Candan's work in [4] to construct arbitrary-order DFT-commuting matrices. Called as the coefficient truncation technique, the coefficient series with length $2k$+1 for the $O(h^{2k})$ approximation to the second derivative were truncated to the length-N dominant coefficient series, based on which the $N \times N$ $O(h^{2k})$ generating matrix was then constructed. The coefficient truncation technique was also employed to construct the n-diagonal arbitrary-order DFT-commuting matrices. Computer experiments were performed to demonstrate superiority of the HGL eigenvectors computed from the arbitrary-order DFT-commuting matrices proposed in this paper. Discrete fractional Fourier transform based on arbitrary-order DFT-commuting matrices introduced in this paper will produce accurate sample approximations of the continuous fractional Fourier transform.

5. REFERENCES

[1] C. Candan, M. A. Kutay, and H. M. Ozaktas, "The discrete fractional Fourier transform," *IEEE Trans. Signal Process.*, vol. 48, no. 5, pp. 1329-1337, May 2000.

[2] S. C. Pei, W. L. Hsue, and J. J. Ding, "Discrete fractional Fourier transform based on new nearly tridiagonal commuting matrices," *IEEE Trans. Signal Processing*, vol. 54, no. 10, pp. 3815-3828, Oct. 2006.

[3] B. W. Dickinson and K. Steiglitz, "Eigenvectors and functions of the discrete Fourier transform," *IEEE Trans. Acoust., Speech, Signal Process.*, vol. 30, no. 1, pp. 25-31, Feb. 1982.

[4] C. Candan, "On higher order approximations for Hermite-Gaussian functions and discrete Fractional Fourier transforms," *IEEE Signal Processing Letters*, vol. 14, no. 10, pp. 699-702, Oct. 2007.

[5] M. A. Kutay, H. M. Ozaktas, O. Arikan, and L. Onural, "Optimal filtering in fractional Fourier domains," *IEEE Trans. Signal Processing*, vol. 45, pp. 1129-1143, July 1997.

[6] S. C. Pei and W. L. Hsue, "The multiple-parameter discrete fractional Fourier transform," *IEEE Signal Processing Letters*, vol. 13, no. 6, pp. 329-332, June 2006.

[7] H. M. Ozaktas, Z. Zalevsky, and M. A. Kutay, *The Fractional Fourier Transform with Applications in Optics and Signal Processing*. New York, John Wiley & Sons, 2000.

[8] W. F. Trench, "Characterization and properties of matrices with generalized symmetry or skew symmetry," *Linear Algebra Appl.*, vol. 377, pp. 207-218, 2004.

[9] C. Candan, "Discrete fractional Fourier transform," M.S. thesis, Bikent Univ., Ankara, Turkey, 1998.